doi:10.1006/jmbi.2001.4673 available online at http://www.idealibrary.com on IDEAL® *J. Mol. Biol.* (2001) **310**, 271–280

JMB

Solution-state NMR Investigations of Triosephosphate Isomerase Active Site Loop Motion: Ligand Release in Relation to Active Site Loop Dynamics

Sharon Rozovsky[1], Gerwald Jogl[2], Liang Tong[2] and Ann E. McDermott[1]*

[1]*Department of Chemistry and*

[2]*Department of Biology Columbia University, New York, NY 10027, USA*

**Corresponding author*

Product release is partially rate determining in the isomerization reaction catalyzed by Triosephosphate Isomerase, the conversion of dihydroxyacetone phosphate to D-glyceraldehyde 3-phosphate, probably because an active-site loop movement is necessary to free the product from confinement in the active-site. The timescale of the catalytic loop motion and of ligand release were studied using ^{19}F and ^{31}P solution-state NMR. A 5′-fluorotryptophan was incorporated in the loop N-terminal hinge as a reporter of loop motion timescale. Crystallographic studies confirmed that the structure of the fluorinated enzyme is indistinguishable from the wild-type; the fluorine accepts a hydrogen bond from water and not from a protein residue, with minimal perturbation to the flexible loop stability. Two distinct loop conformations were observed by ^{19}F NMR. Both for unligated (empty) and ligated enzyme samples a single species was detected, but the chemical shifts of these two distinct species differed by 1.2 ppm. For samples in the presence of subsaturating amounts of a substrate analogue, glycerol 3-phosphate, both NMR peaks were present, with broadened lineshapes at 0 °C. In contrast, a single NMR peak representing a rapid average of the two species was observed at 30 °C. We conclude that the rate of loop motion is less than 1400 s^{-1} at 0 °C and more than 1400 s^{-1} at 30 °C. Ligand release was studied under similar sample conditions, using ^{31}P NMR of the phosphate group of the substrate analogue. The rate of ligand release is less than 1000 s^{-1} at 0 °C and more than 1000 s^{-1} at 30 °C. Therefore, loop motion and product release are probably concerted and likely to represent a rate limiting step for chemistry.

Keywords: triosephosphate isomerase; protein dynamics; flexible loop; chemical exchange; 5′-fluorotryptophan

Introduction

Triosephosphate isomerase, a glycolytic enzyme, catalyses the reversible isomerization of dihydroxyacetone phosphate to D-glyceraldehyde 3-phosphate. Although both species are produced by aldolase in equal amounts, only D-glyceraldehyde 3-phosphate will be further utilized in the glycolytic pathway. The direction from dihydroxyacetone phosphate to D-glyceraldehyde 3-phosphate (thermodynamically unfavorable) has particular biological relevance as DHAP accumulation disrupts the regulation of normal cell functions, leading to chronic hemolytic anemia and neuromuscular disorders (Schneider, 2000).

A remarkably well-studied system, its relatively simple chemical reaction offers much insight into the connection between form and function (Alber *et al.*, 1981; Albery & Knowles, 1976; Knowles, 1991). The reaction free energy profile, determined by Albery and Knowles (1976), indicates that product release is the rate determining step (or one of the rate-limiting

Abbreviations used: TIM, triosephosphate isomerase; DHAP, dihydroxyacetone phosphate; GAP, D-glyceraldehyde 3-phosphate; G3P, DL-glycerol 3-phosphate.

E-mail address of the corresponding author: aem5@columbia.edu

0022-2836/01/010271–10 $35.00/0

steps) in the thermodynamically unfavorable but biologically significant direction (dihydroxyacetone phosphate as the substrate). In contrast, in the thermodynamically favorable direction (D-glyceraldehyde 3-phosphate as substrate) the rate determining step is the proton transfer to the reaction intermediate to form the product. The strict sequence conservation of a flexible active-site loop suggests an indispensable role for motion in the reaction mechanism. The active-site loop participates in the chemical catalysis by organizing the catalytic triad, protecting the reaction chemical intermediates in the closed state, and allowing for binding and release in the open state (Pompliano *et al*., 1990; Sampson & Knowles, 1992a).

NMR has a rich history in comprehension of the isomerization mechanism, including the determination of protonation states of active-site residues (Browne *et al*., 1976; Hartman & Ratrie, 1977; Lodi & Knowles, 1991), the ionization state and hydration of ligands (Belasco *et al*., 1978; Hartman *et al*., 1975; Jones & Waley, 1979; Webb *et al*., 1977), the characterization of low barrier short hydrogen bonds (Harris *et al*., 1997), and measurements of ligand dissociation kinetics (Campbell *et al*., 1979). The phosphate β-elimination, an important side reaction, was discovered in ^{1}H NMR investigations of the substrate-enzyme complex (Browne *et al*., 1976) and later explored by ^{31}P NMR (Campbell *et al*., 1979). Kinetic parameters of the protein motion have been measured using both solid-state (Rozovsky & McDermott, 2001; Williams & McDermott, 1995) and solution-state NMR (Loria *et al*., 1999; Yuksel *et al*., 1994). Measurement of a unique conformational change, such as loop motion, requires the distinction of only one specific functionally significant motion above the collection of thermally accessible motions. The timescale of the protein's biologically relevant motions is probably defined by the choice of sample conditions such as ligands, ionic strength, and temperature. According to the kinetic isotopic exchange experiments, the rate of TIM conformational change is clearly influenced by the chemical properties of the substrate. The conversion of dihydroxyacetone phosphate to D-glyceraldehyde 3-phosphate by TIM occurs with a catalytic rate $k_{cat} = (7.5 \pm 0.2) \times 10^2$ s^{-1}, a substrate-binding constant $K_m = 1.4 \pm 0.1$ mM, and the rate limiting step appears to be a slow conformational change according to the isotope data. In the reverse direction $k_{cat} = (8.7 \pm 0.3) \times 10^3$ s^{-1}, $K_m = 0.055(\pm 0.004)$ mM, and the rate limiting step is the proton transfer (Nickbarg & Knowles, 1988). Therefore, loop opening on DHAP must be faster than 8×10^3 s^{-1}, but on GAP it must be comparable to 7×10^2 s^{-1}. It can be presumed that the much tighter binding of GAP presents a higher activation energy to loop opening; implying that the loop will remain closed during the duration time of the reaction tightly bound intermediates and transition state species, preventing interruption of chemistry by sudden solvation. Naturally, it is of interest to study the loop motion during actual catalysis, unfortunately the elimination of phosphate from the substrate and consequently enzyme modification by the highly reactive product methylglyoxal (Degenhardt *et al*., 1998) has complicated NMR experiments in the presence of the substrate near functional temperature. Instead, we have examined the influence of a substrate analogue on the loop rate. The binding affinity of glycerol 3-phosphate (G3P) is similar to that of DHAP. K_i is 1.4(±0.3) mM (Nickbarg & Knowles, 1988). In additional chemical details G3P closely resembles the substrates, and therefore this system was characterized in the most detail. The system was otherwise poised at conditions (pH, ionic strength, etc.) to maximize enzymatic activity (Lambeir *et al*., 1987; Putman *et al*., 1972).

The conformational timescales of the active-site loop in the presence of a substrate analogue were probed using a single tryptophan reporter in the loop's N-terminal hinge of a yeast TIM mutant, Trp90Tyr Trp157Phe. The kinetic parameters of the mutant, used in investigations of the time scale of the flexible loop motion (Loria *et al*., 1999; Rozovsky & McDermott, 2001; Sampson & Knowles, 1992b; Williams & McDermott, 1995), hardly differ from those of the wild-type yeast TIM. Crystallographic studies were employed to validate the structural integrity of the TIM mutant and examine possible influences on the flexible loop stability induced by the fluorine atom. The ^{19}F nucleus offers a particularly sensitive probe of molecular environment. Incorporation of fluorine into proteins rarely perturbs either the protein structure or kinetic properties except for cases in which the fluorinated residue is a part of the active-site (Gerig, 1994). The van der Waals radius of fluorine (1.47 Å) is not much larger than that of a proton (1.20 Å) and steric hindrance is not a concern. Fluorine in organic compounds is a poor hydrogen bond acceptor (Howard *et al*., 1996); its hydrogen bond acceptor capability and the increased dipole moment (3.6 D for 5′-fluoroindole *versus* 2.1 D for the indole) can have interesting effects. For example conductance of Gramicidin A channels increased as a consequence of 5′-fluorotryptophan substitutions (Andersen *et al*., 1998). Glutathione transferase containing 5′-fluorotryptophan has increased turnover rate due to enhanced dissociation constant (Parsons *et al*., 1998). In Annexin V, where 4, 5, and 6 fluorotryptophan residues were incorporated into a single tryptophan location that mediates Ca^{2+} binding, binding to membrane was three, two times less and three times higher than the unlabeled protein (Minks *et al*., 1999). The pK_a shift for a 4-fluorohistidine incorporated in a catalytic position of bovine ribonuclease

abolished activity (Taylor *et al*., 1981). Unless the labeled residue is involved directly in the details of the biological function, perturbation is typically minimal. In TIM, the fluorine label resides at the loop N terminal hinge, an absolutely conserved region associated with the catalytic base conformational change. The tryptophan position is 8 Å away from the active-site with the fluorine label pointing away from the ligand binding site; it is unlikely to either effect or sense directly ligand binding and dissociation. The tryptophan swings by about 45° between the open and closed loop conformation (Lolis & Petsko, 1990); the stability of the open *versus* closed conformations can be altered if the fluorine contacts another protein residue as its hydrogen bond partner. In both conformations the tryptophan is relatively close to loop 5, in particular Lys134 side-chain which is within van der Waals contact with the indole ring π-electrons, and to loop 6 backbone, where the amide of Leu174 is in close proximity to the indole ring of the tryptophan residue.

In the accompanying paper (Rozovsky & McDermott, 2001) we have provided experimental evidence using broadline deuterium solid state NMR for large angle motions of a tryptophan probe located at the active-site loop N-terminal hinge. These two reports serve to define the timescale of the loop motion under functioning conditions. In the following we describe ^{19}F and ^{31}P solution NMR studies of the time scale of loop motion and ligand release. In particular, the relation between ligand release, the catalytic loop motion and the influence of ligation on the population ratio of the flexible loop conformations. These papers also constitute a detailed comparison between solution and solid state chemical exchange measurements by NMR. Despite the biases of the methods and the important differences in sample conditions, similar conclusions about the loop time scale can be reached by the two methods.

Results

The structure of the 5′-fluorotryptophan incorporated at position 168

The crystal structure of the yeast TIM mutant (Trp90Tyr Trp157Phe with 5′-fluorotryptophan at Trp168) was determined at 1.8 Å resolution (Table 1). The two independent monomers of the enzyme in the crystal have essentially the same conformation, with rms distance of 0.24 Å for all equivalent atoms between the two monomers. The crystals of the mutant are isomorphous to that of the wild-type yeast TIM. The structure of the mutant is virtually identical to that of the wild-type unligated enzyme. The rms distance between equivalent main-chain atoms of the two structures is 0.3 Å. The active-site flexible loop containing the 5′ Fluorotryptophan at Trp168 residue has the same conformation in the two structures (Figure 1(a)). There is clear electron density for the fluorine atom (Figure 1(b)), and the crystallographic analysis suggests that the occupancy of this fluorine position is about 60 %. This appears to be consistent with mass spectrometry analysis on the protein samples, which suggests a fluorine incorporation percentage of about 50 %.

Table 1. Summary of crystallographic information

Space group	$P2_1$
Cell	$a = 60.60$ Å
	$b = 97.06$ Å
	$c = 49.25$ Å
	$\beta = 91.70°$
Frames	132
Observations	152,637
Unique reflections	50,459
R-merge	0.073
Resolution range for refinement	30-1.8 Å
Observed reflections for refinement	50,392
Completeness	95.4 %
R-factor	0.175
R-free	0.208
rms deviation	
Bond lengths (Å)	0.005
Bond angles (deg.)	1.2
Protein residues (atoms)	496(3758)
Solvent atoms	629

The indole ring of Trp168 is located in the same position as in the wild-type enzyme (Figure 1(a)). Both the aromatic packing with Tyr164 and Pro166 and the coordination of the N-terminal hinge with loop 5 Glu129 are maintained in the mutant. The fluorine atom on the indole ring forms a hydrogen-bond to a solvent water molecule (Figure 1(b)). There are no contacts from this fluorine atom to the enzyme, suggesting that the introduction of the fluorine atom should not affect the stability of the active-site flexible loop (loop 6).

The other two changes of the enzyme in the mutant studied here (Trp90Tyr and Trp157Phe) did not disturb the structure either. The hydroxyl of Tyr90 is within hydrogen-bonding distance of the side-chain of Glu37. However, this new interaction did not disrupt the ion-pair interactions between Glu37 and Arg205 that is already present. At the other mutation site, the indole nitrogen atom of Trp157 makes a hydrogen-bond to the main chain of Ala154 in the wild-type enzyme. In the Phe157 mutant, this hydrogen bond is lost, but the Ala154 residue is still located at the same position.

The flexible loop in the active-site (loop 6) of TIM is involved in crystal packing interactions in the crystal form studied here. However, solid-state NMR studies showed that the loop can still undergo the open-closed conformational transition in this crystalline state. Preliminary crystallographic studies with single crystals also support of the SSNMR observations, showing that loop 6 can adopt the closed conformation in the crystal lattice.

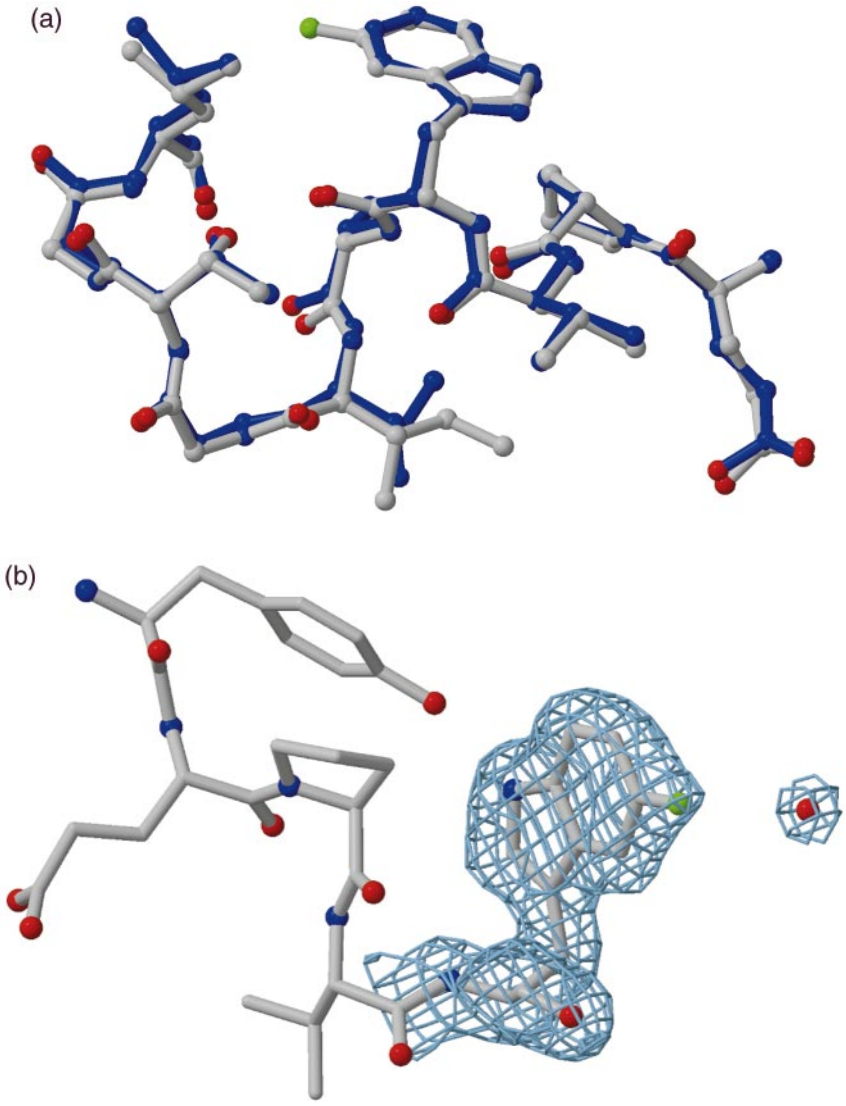

Figure 1. (a) The superposition of loop 6 from both the wild-type yeast TIM structure (PDB entry 1YPI (Lolis *et al.*, 1990)) and the Trp90Tyr Trp157Phe with 5′-fluorotryptophan incorporated at position 168 are shown. Loop 6 backbone is identical in both structures. A slight variation is found in Ile170 side-chain, which is not unusual for a solvent exposed side-chain. (b) The electron density of the 5′-fluorotryptophan incorporated into a single location on TIM's flexible loop is shown. The presence of the fluorine atom does not modify the hydrophobic packing and hydrogen bonding interactions observed for the unmodified tryptophan in the wild-type yeast TIM (Lolis *et al.*, 1990). A water molecule is within hydrogen bond distance from the fluorine atom in both subunits. Graphical representations were prepared with the program MOLSCRIPT (Kraulis, 1991) and RASTER3D (Merritt & Bacon, 1997).

Active site loop time scale of motion

NMR spectra of 5′-fluorotryptophan in position 168 can be used as a marker for the conformation of the loop in the presence and absence of a substrate analogue. Figure 2 shows spectra at two limiting temperatures, collected at NMR field strengths of 7.05 and 9.4 T. The spectrum of the unligated state has only one resonance whose position does not shift substantially over the temperature range employed. A 0.3 ppm shift upfield upon decreasing the temperature to 0 °C is analogous to the 0.2 ppm observed for the free 5′-fluorotryptophan in 10 % $^{2}H_2O$ over the same temperature range; fluorine chemical shifts are known to be sensitive to both temperature and solvation (Hansen *et al.*, 1985). The absence of other resonances for either the closed loop conformation or other closely related conformations of the open conformations are attributed to relatively skewed population ratio and fast exchange. When saturating amounts of the substrate analogue, DL-glycerol-3-phosphate, was added, the fluorine resonance shifted by 1.2 ppm upfield. The distance of the fluorine label in the bound form should be about 10 Å away from the ligand based on the wild-type yeast structure (Davenport *et al.*, 1991); therefore, the fluorine chemical shift is probably responding

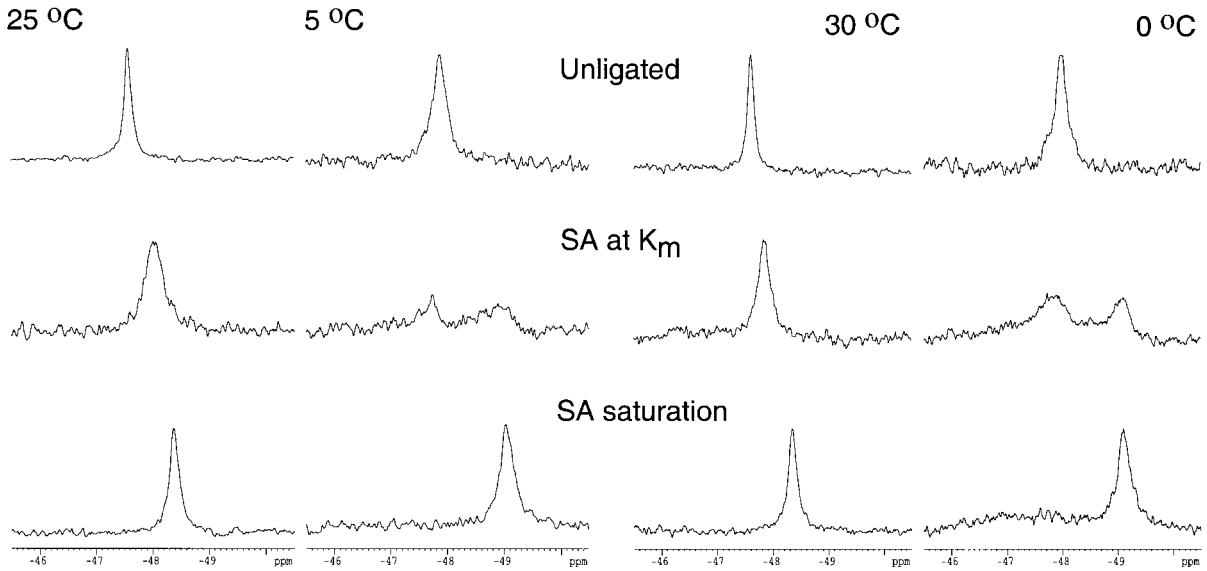

Figure 2. ^{19}F NMR line shape of 5′-fluorotryptophan in yeast TIM Trp90Tyr Trp157Phe which has a single remaining tryptophan residue at position 168, located in the N-terminal hinge of loop 6. No proton decoupling was employed. On the left, line shapes of the unligated, subsaturated (1.2 mM G3P) and saturated (10 mM G3P) enzyme at 25 °C and 5 °C at 7.05 T using 1.2 mM TIM in 50 mM Tris-HCl, 50 mM NaCl (pH 6.8) at 25 °C. On the right, lineshapes at similar sample conditions at 30 °C and 0 °C at 9.4 T. The amount of enzyme and transients in each magnetic field data set was kept constant (but for spectra at 0 °C 1.2 mM G3P which was acquired with twice the number of transients), therefore variation in signal-to-noise emanate from the effect of motion. In unligated samples, ^{19}F shifts of about 47.5 ppm and line widths of 35 and 45 Hz are seen when the sample temperature is 25 °C (at 7.05) *versus* 30 °C (at 9.4 T). In ligated (saturated) enzymes the ^{19}F resonance shifts to 48.4 ppm and line widths of 41 and 67 Hz are seen at temperature of 25 °C (at 7.05) *versus* 30 °C at (9.4 T). The change in chemical shift upon binding is presumably related to the aromatic packing of Trp168 with Tyr164 and Pro166 in the free state and partial solvent exposure in the ligand bound state. In partially saturated enzyme, the behavior is markedly different at low temperatures (0 and 5 °C), where two separate broad peaks for free and bound species are seen, as compared with higher temperatures (25 or 30 °C) where a single motionally averaged peak is observed. The peak intensity and integral suggest equal population for both loop conformations the shifts are separated by 1.2-1.3 ppm. At higher temperatures, the fast average is located half way between the two limiting states, at 47.85 ppm and 9.4 T and 48.0 ppm for 7.05 T with a broad line width of about 110 Hz. From this observation we conclude that the loop opening rate is slower than 1400 s^{-1} at 0 °C and faster than 1400 s^{-1} at 30 °C.

to the protein conformational change rather than directly to the ligand presence. The shift is associated with an environmental change: in the unligated state the indole ring is packed with Tyr164 and Pro166, and loop closure rotates the indole ring above the loop plane, altering its interactions with the neighboring aromatic residues. We logically associate the downfield peak with the open structure, and the upfield peak with the closed conformation observed by X-ray crystallography.

The fluorine chemical shift change offers a tool for documenting the rate of loop motion *via* chemical exchange type effects. If a simple two site model can be assumed, broadening and coalescence will occur when the rates of loop opening and/or closing are of the order of the difference in frequency of the two sites, i.e. 1400 s^{-1}. Information about the conformational change can be related to the rate of reaction turnover for the two substrates (8000 and 800 s^{-1}). The rate constant for opening is most easily detected when the open and closed populations are nearly equal. Therefore, a solution of the enzyme with subsaturating amounts G3P was investigated. At 0 °C two resolved peaks, with roughly the same intensity, were observed for half saturated samples and allowed us to confirm the population ratio. The peaks appeared at the chemical shift values of the fully saturated and the unligated enzyme peaks, but clearly broadened. At 30 °C a spectrum with a single peak at the population weighted average of the two chemical shifts was observed, with a broadened line width. We conclude that coalescence, with an opening rate of about 1400 s^{-1}, occurs at about 10 °C. The following conclusions emerge: (i) the loop's conformation clearly responds to the ligand concentration in rough qualitative agreement with its K_i value and validates the notion that every bound enzyme has its loop closed; (ii) the loop opening and closing timescale is of order 3000-5000 s^{-1} near room temperature; (iii) the rate responds strongly to temperature.

The line widths and spin lattice relaxation rates for the loop, in both the open and the closed (or

ligated) state qualitatively indicate a great degree of mobility (''fast limit'' motions) for this site. If the relaxation were due entirely to rigid protein tumbling with a correlation time of 20 ns and the fluorine's CSA as a dominant term (ca 100 ppm), spin lattice relaxation rates of less than 0.1 s^{-1} and dephasing times of more than 300 s^{-1} would be expected. In contrast, for the unligated enzyme resonance the observed line widths were narrowed (35 Hz at 7.05 T and 45 Hz at 9.4 T, both measured without proton decoupling) and spin-lattice relaxation rates were enhanced. Spin lattice relaxation values, T_{1Z} at 7.05 T is 0.7(±0.1) second for the unligated state and 0.5(±0.2) second in the presence of phosphate or G3P, are indicative of order parameters less than about 0.7. We did not attempt a quantitative treatment of the order parameter for this site. Our limited data sets do not allow us to deconvolve chemical exchange from rapid dephasing reliably. Our deuterium dynamics data indicate that the local motions are likely to include terms that are on the same order as the sample tumbling. It is clear that the tryptophan marker on the loop has local mobility, in agreement with the conclusions from our broadline deuterium SSNMR studies, both lineshape at low temperature (Rozovsky & McDermott, 2001) and relaxation measurements (Rozovsky, 2000).

The rate of ligand release was also measured in this temperature range, exploiting the fact that the ^{31}P resonance condition differs between the bound *versus* the free ligand form. Only the D-enantiomer binds appreciably to the enzyme; the unbound L-enantiomer provides an internal marker for the free ligand spectrum. G3P binding is independent of pH over the range 6.5-8.5 (Campbell *et al.*, 1979; Jones & Waley, 1979), and both the monoanion and dianion of D-G3P bind to the enzyme; variation in ligand binding efficiency is not expected over the temperature range and sample conditions employed in these studies. ^{31}P NMR spectra at 14.1 T, of 5.75 and 1.2 mM G3P (which are approximately 5 K_i and K_i, respectively) in the presence of 2.1 mM TIM (4.2 mM active-sites) at 0 °C and 30 °C are presented in Figure 3. At 30 °C in the presence of 5.75 mM G3P, two peaks are observed corresponding to the free L-G3P at 5.50 ppm with 20 Hz line width, and an enzyme bound D-G3P at 6.35 ppm with 52 Hz line width. The D-enantiomer appears to be in fast exchange between its free and bound forms: when the enzyme sample is titrated with respect to substrate concentration, the chemical shift of the peak attributed to the D-enantiomer moves according to a population weighted average of the bound and free forms. In contrast, at 0 °C the peak position for the bound D-enantiomer is fixed but its intensity changes as if chemical exchange between the free and bound forms is in the slow limit. Separation between the bound and free forms is 1.3 ppm. We conclude that ligand release is faster than 1000 s^{-1} at 30 °C and much slower than 1000 s^{-1} at 0 °C. The ligand release and the loop motion have comparable timescales within the error of our measurement, and both exhibit strong temperature dependence. The timescale is also in agreement with loop motion rate estimated from broadband deuterium SSNMR. It is probable, based on these results, that they represent one concerted process.

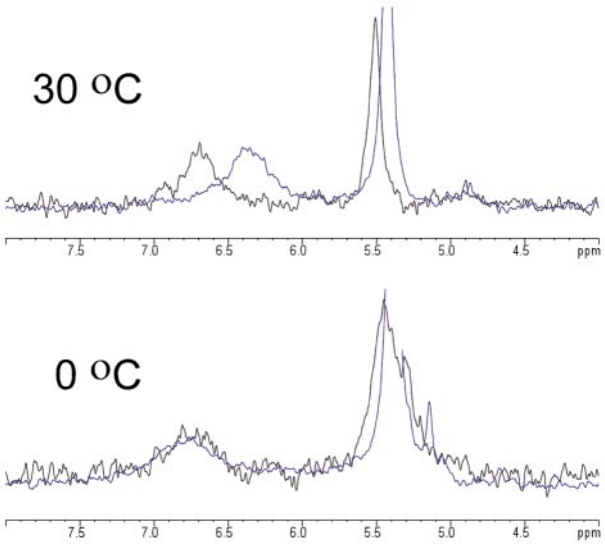

Figure 3. ^{31}P NMR spectra of G3P titrations of samples containing 2.1 mM TIM (4.2 mM active-site concentration, 50 mM Tris-HCl, 50 mM NaCl, pH 6.8 at 25 °C) at 14.1 T, collected with a 2 kHz proton decoupling field. In blue, 5.75 mM G3P, at 30 °C the free L enantiomer resonance at 5.45 ppm with 18 Hz line width, the bound D enantiomer is 0.9 ppm downfield from the free L enantiomer, with a 50 Hz line width. At 0 °C the chemical shift separation is 1.3 ppm. In black, 1.2 mM G3P, the two enantiomers are 1.2 ppm apart at 30 °C and 1.3 ppm at 0 °C. The ligand release is thus faster then 1000 s^{-1} at 30 °C.

Discussion

The chemical exchange phenomena observed for the loop conformation was simulated using a kinetic model in which three forms of the enzyme are at equilibrium: the unbound enzyme, an encounter complex with a ligand bound and an open loop and a ligand bound enzyme with a closed loop (Scheme 1). The enzyme loop conformation is limited to the two crystallography observed states:

$$E + S \underset{k_{diss}}{\overset{k_{asso}}{\rightleftarrows}} ES_{open} \underset{k_{open}}{\overset{k_{close}}{\rightleftarrows}} ES_{close}$$

open and closed.

Based on suppression of the phosphate elimination reaction (Richard, 1991), active-site shielding as observed by isotopic trapping (Rose *et al.*, 1990) and by hydrogen exchange experiments (Browne

& Waley, 1974) we can put an estimate on the ratio k_{close}/k_{open} of above 100 for G3P. Therefore, we can further constrain the simulations on the basis of the equation:

$$K_d = \left(\frac{k_{diss}}{k_{asso}}\right)\left(\frac{k_{close}}{k_{open}}\right)$$

Assuming k_{asso} is diffusion limited, a value 1×10^6 M^{-1} s^{-1} is in agreement with the sample conditions (1.2 mM to 10 mM G3P). K_{diss} was adjusted according to G3P K_d. Data from experiments conducted at both magnetic fields were used to test the model. For the two resolved peaks observed at 0 °C in the presence of 1.2 mM G3P a value of 1000 s^{-1} was estimated for the loop opening since the loss of intensity and considerable line broadening indicated conditions close to but slower than coalescence. The population ratio of the closed loop enzyme and the encounter complex were kept at a ratio of a 100 (loop closing 1×10^5 s^{-1}) while the populations of the unligated and closed-loop-enzyme were essentially equal. The implicit assumption is that the encounter complex is sparsely populated and that its chemical shifts are identical to the unligated enzyme, as the loop remains open in spite of substrate binding. Accelerating the rate of loop opening to 5000 s^{-1} at 30 °C resulted in a broad peak whose averaged position, line width and intensity agree well with the experimental data (Figure 4).

For samples containing 10 mM G3P approximately 85 % percent of the enzyme is bound. Therefore, the population of the unligated *versus* ligated enzyme were adjusted accordingly, keeping a 1 % population of the encounter complex. This simplification is convenient but probably inaccurate: at 4 °C the elimination of phosphate is much reduced, suggesting a change not only in rates but also in populations and the enzymatic catalysis (Campbell *et al.*, 1979). Using the same rates as for the 1.2 mM G3P sample the trend in line width, line position and intensity is reproduced. The major features of the data are clearly in agreement with the simulations.

Conclusions

Studies of the kinetics of TIM active-site loop and of the ligand release suggest a rate determining step involving a concerted loop opening motion and ligand release. The opening rate is above 1400 s^{-1} at room temperature when DL-glycerol-3-phosphate is used as a substrate surrogate and is strongly temperature dependent. ^{31}P NMR spectra, serving as reporters of ligand off-rates, point to a similar rate. These studies employ a fluorinated single tryptophan in the N-terminal hinge as a reporter; X-ray crystallographic investigations of this chemically modified mutant enzyme indicate that it is essentially indistinguishable from the wild-type structure. The opening rate depends on the choice of ligand: stronger binding ligands exhibits slower opening rates, as expected. The good agreement between these measurements and others made in the solid state under different conditions lend credibility to the notion that loop opening step is partially rate determining, independent of the details of the sample condition. The loop motion rate is ligand dependent, suggesting that this rate was optimized for function in the presence of the substrate.

Materials and Methods

All reagents used were purchased from Sigma-Aldrich Co. with the exception of glycerol-3-phosphate dehydrogenase, which was purchased from Boehringer Mannheim Ltd., ^2H_2O from Cambridge Isotope Laboratories Inc. G3P and L-G3P were obtained from both Fluka and Sigma.

Preparation of yeast mutant triosephosphate isomerase

Protein expression and purification were described in the preceding paper (Rozovsky & McDermott, 2001). The selected medium contained 40 mg/ml DL-5′-fluorotryptophan. Incorporation ratio was evaluated by electrospray Q-TOF mass spectrometric analysis, conducted by the HHMI Protein Core Facility at the College of Physicians and Surgeons, Columbia University.

Activity assays

Activity assays were conducted as described by Putman & Knowles (1972; Putman *et al.*, 1972). The fluorinated enzyme V_{max} is hardly affected by the fluorine incorporation.

NMR samples

Solution-state NMR samples typically contained 20 mg TIM in 50 mM Tris-HCl, 50 mM NaCl, 1 mM EDTA, 10 % ^2H_2O (v/v) pH 6.8 at 25 °C (uncorrected) in a volume of 400 µl.

NMR spectroscopy

NMR spectra were acquired on a Bruker DPX 300, DRX 400 and DRX 600. DRX600 is located in the biochemistry and molecular biophysics department, Columbia University. ^{19}F spectra (282 MHz) were collected using a 90° pulse width of 9.1 µs, acquisition time four seconds, pulse delay three to four seconds; no proton decoupling was employed. The number of transients in each spectrum is about 4000. T_{1Z} relaxation measurements yielded values between 0.5-0.7 seconds. ^{19}F spectra at 376 MHz were collected using a 90° pulse width of 10 µs, acquisition time of two seconds, pulse delay 0.5 seconds; no proton decoupling was employed. The number of transients in each spectrum is about 14,000. Relatively long pulse delays were employed for all enzyme samples acquired at 7.05 T to prevent a bias in sampling alternative loop conformations. Exponential line broadening of 10 Hz was applied to the time domain data, and 8000 experimental points were included. ^{19}F chemical shifts were referenced to neat external trifluoroacteic

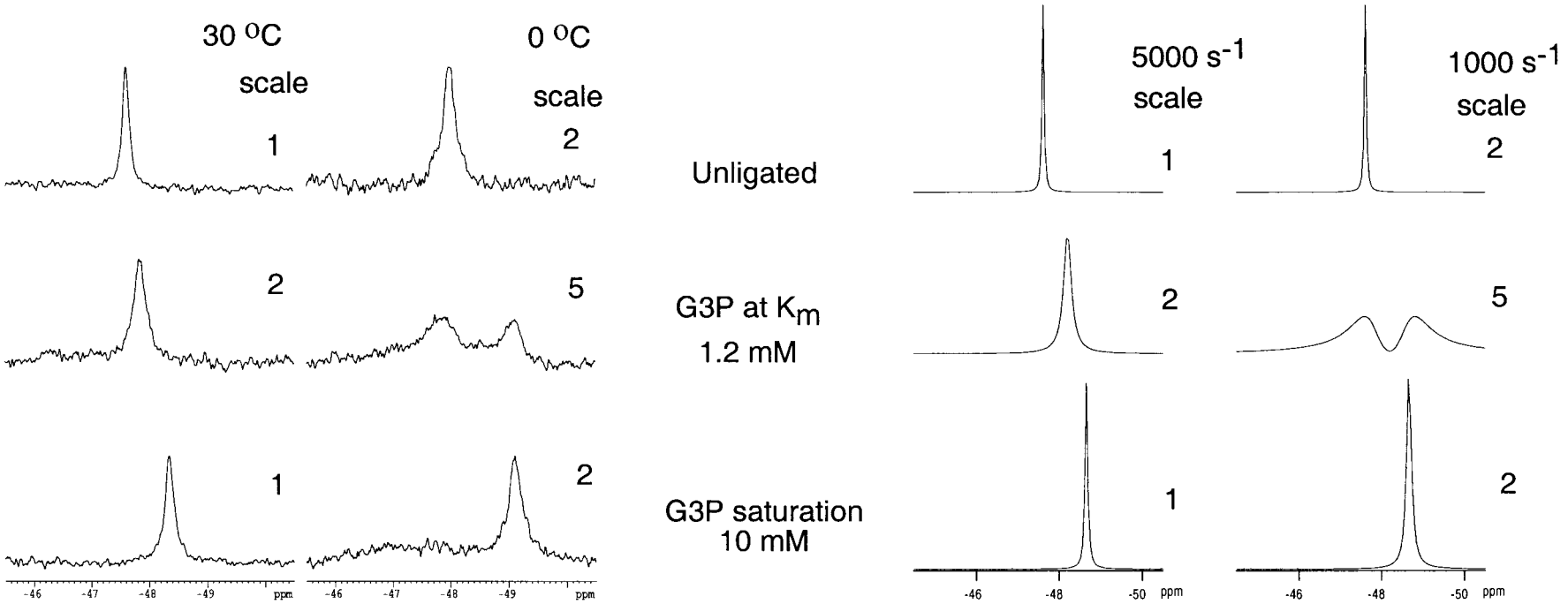

Figure 4. Lineshape simulations for the flexible loop 5′-fluorotryptophan ^{19}F resonance (at 9.4 T, Figure 2 right panel, reproduced for convenience on the left). The unligated state can be simulated with two sites corresponding to the open and closed loop's conformation, at any arbitrary skewed populations, assuming that the unligated enzyme is not likely to close on an unligated active-site. Loop motion in the present of G3P was simulated using a three site model and constraint from kinetic data. Loop opening rate is 1000 s^{-1} at 0 °C and 5000 s^{-1} at 30 °C. Line broadening used in the simulation is 10 Hz. The T_2-induced linewidth is certainly borader, but has not been considered here. Populations of the loop conformations were selected based on sample conditions; the encounter complex occupancy is assumed to be 1 % of the closed loop enzyme occupancy. Simulations are scaled in a manner analogous to the experimental data.

acid at 0 ppm at 25 °C (free 5′-fluorotryptophan is −49.5 ppm relative to TFA).

Broad-band proton decoupled ^{31}P NMR spectra were measured at a Larmor frequency of 121, 160 and 242 with pulse length of 7.6 μs (30 °), 11.75 μs (30 °) and 8.5 μs (90 °), respectively. Acquisition times were 2.5 seconds and a 0.5 second pulse delay was utilized. Line broadening of 2-4 Hz was applied to the time domain data using 16 K points. ^{31}P chemical shifts were referenced to external 85 % phosphoric acid at 0 ppm at 25 °C.

Crystallography

Crystallization of yeast TIM mutant, Trp90Tyr Trp157Phe in which a 5′-fluorotryptophan was incorporated at position 168 was by batch methods as described before (Rozovsky & McDermott, 2001). In brief, a solution containing 40 mg/ml protein in 50 mM Tris-HCl, 50 mM NaCl, 1 mM EDTA, pH 6.8 at 25 °C, was crystallized at room temperature with 14-16 % polyethylene glycol (average molecular weight 4000). Crystals appeared within a few hours and grew to about 0.3 mm × 0.3 mm × 0.1 mm.

Data collection

X-ray diffraction data up to 1.8 Å resolution were collected on a rotating anode X-ray generator (MSC). The crystal was flash frozen in liquid N_2 and maintained at 100 K during data collection. The oscillation range per image was 1.5 ° and the exposure time was 20 minutes. Diffraction images were recorded on an RAxisIV detector and processed with the HKL package (Otwinowski & Minor, 1997) Crystals belong to space group $P2_1$ with cell dimensions $a = 60.6$ Å, $b = 97.1$ Å, $c = 49.3$ Å, $\beta = 91.7$ °.

Refinement

Crystals of the 5′-fluorotryptophan 168 mutant of TIM are isomorphous to wild-type TIM crystals (open loop conformation, PDB accession code: 1YPI). Coordinates from the wild-type TIM structure were used as initial model. NCS restrained rigid body refinement and simulated annealing refinement using torsional angle dynamics were carried out with the program CNS (Brunger *et al.*, 1998). The two monomers were refined independently during further refinement cycles. Side-chain conformations and the flexible loop region (residues 165 to 177) were fitted with the program O (Jones *et al.*, 1991). Solvent molecules were identified from a difference electron density map as peaks that have reasonable hydrogen bonding partners. The refinement statistics are summarized in Table 1.

Protein Data Bank access code

The atomic coordinates of the structure have been deposited with the RCSB Protein Data Bank, accession code 1I45.

Acknowledgments

The authors thank Professor A. G. Palmer III, of Columbia University, for helpful discussions. Acquisition of the DRX600 spectrometer was supported by NSF grant DBI-9601661. This work was supported by National Institutes of Health grant GM49964.

References

Alber, T., Banner, D. W., Bloomer, A. C., Petsko, G. A., Phillips, D., Rivers, P. S. & Wilson, I. A. (1981). On the three-dimensional structure and catalytic mechanism of triose phosphate isomerase. *Philos. Trans. R. Soc. London, ser. B,* **293**, 159-171.

Albery, W. J. & Knowles, J. R. (1976). Free-energy profile of the reaction catalyzed by triosephosphate isomerase. *Biochemistry,* **15**, 5627-5631.

Andersen, O. S., Greathouse, D. V., Providence, L. L., Becker, M. D. & Koeppe, R. E. (1998). Importance of tryptophan dipoles for protein function: 5-fluorination of tryptophans in gramicidin A channels. *J. Am. Chem. Soc.* **120**, 5142-5146.

Belasco, J. G., Herlihy, J. M. & Knowles, J. R. (1978). Critical ionization states in the reaction catalyzed by triosephosphate isomerase. *Biochemistry,* **17**, 2971-2978.

Browne, C. A. & Waley, S. G. (1974). Studies of triosephosphate isomerase by hydrogen exchange. *Biochem. J.* **141**, 753-760.

Browne, C. A., Campbell, I. D., Kiener, P. A., Phillips, D. C., Waley, S. G. & Wilson, I. A. (1976). Studies of histidine residues of triosephosphate isomerase by proton magnetic resonance and X-ray crystallography. *J. Mol. Biol.* **100**, 319-343.

Brünger, A. T., Adams, P. D., Clore, G. M., DeLano, W. L., Gros, P. & Grosse-Kunstleve, R. W. *et al.* (1998). Crystallography & NMR system: a new software suite for macromolecular structure determination. *Acta Crystallog. sect. D,* **54**, 905-921.

Campbell, I. D., Jones, R. B., Kiener, P. A. & Waley, S. G. (1979). Enzyme-substrate and enzyme-inhibitor complexes of triose phosphate isomerase studied by 31P nuclear magnetic resonance. *Biochem. J.* **179**, 607-621.

Davenport, R. C., Bash, P. A., Seaton, B. A., Karplus, M., Petsko, G. A. & Ringe, D. (1991). Structure of the triosephosphate isomerase-phosphoglycolohydroxamate complex: an analogue of the intermediate on the reaction pathway. *Biochemistry,* **30**, 5821-5826.

Degenhardt, T. P., Thorpe, S. R. & Baynes, J. W. (1998). Chemical modification of proteins by methylglyoxal. *Cell. Mol. Biol.* **44**, 1139-1145.

Gerig, J. T. (1994). Fluorine NMR of proteins. *Prog. Nucl. Magn. Reson. Spectrosc.* **26**, 293-370.

Hansen, P. E., Dettman, H. D. & Sykes, B. D. (1985). Solvent-induced deuterium-isotope effects on F-19 chemical- shifts of some substituted fluorobenzenes: formation of inclusion complexes. *J. Magn. Reson.* **62**, 487-496.

Harris, T. K., Abeygunawardana, C. & Mildvan, A. S. (1997). NMR studies of the role of hydrogen bonding in the mechanism of triosephosphate isomerase. *Biochemistry,* **36**, 14661-14675.

Hartman, F. C. & Ratrie, H. D. (1977). Apparent equivalence of the active-site glutamyl residue and the essential group with pK_a 6.0 in triosephosphate isomerase. *Biochem. Biophys. Res. Commun.* **77**, 746-752.

Hartman, F. C., LaMuraglia, G. M., Tomozawa, Y. & Wolfenden, R. (1975). The influence of pH on the interaction of inhibitors with triosephosphate iso-

merase and determination of the pK_a of the active-site carboxyl group. *Biochemistry,* **14**, 5274-5279.
Howard, J. A. K., Hoy, V. J., Ohagan, D. & Smith, G. T. (1996). How good is fluorine as a hydrogen bond acceptor? *Tetrahedron,* **52**, 12613-12622.
Jones, R. B. & Waley, S. G. (1979). Spectrophotometric studies on the interaction between triose phosphate isomerase and inhibitors. *Biochem. J.* **179**, 623-630.
Jones, T. A., Zou, J. Y., Cowan, S. W. & Kjeldgaard, M. (1991). Improved methods for building protein models in electron- density maps and the location of errors in these models. *Acta Crystallog. sect. A,* **47**, 110-119.
Knowles, J. R. (1991). Enzyme catalysis: not different, just better. *Nature,* **350**, 121-124.
Kraulis, P. J. (1991). MOLSCRIPT: a program to produce both detailed and schematic plots of protein structures. *J. Appl. Crystallog.* **24**, 946-950.
Lambeir, A. M., Opperdoes, F. R. & Wierenga, R. K. (1987). Kinetic-properties of triose-phosphate isomerase From trypanosoma-brucei-brucei - a comparison with the rabbit muscle and yeast enzymes. *Eur. J. Biochem.* **168**, 69-74.
Lodi, P. J. & Knowles, J. R. (1991). Neutral imidazole is the electrophile in the reaction catalyzed by triosephosphate isomerase: structural origins and catalytic implications. *Biochemistry,* **30**, 6948-6956.
Lolis, E. & Petsko, G. A. (1990). Crystallographic analysis of the complex between triosephosphate isomerase and 2-phosphoglycolate at 2.5 Å resolution: implications for catalysis. *Biochemistry,* **29**, 6619-6625.
Lolis, E., Alber, T., Davenport, R. C., Rose, D., Hartman, F. C. & Petsko, G. A. (1990). Structure of yeast triosephosphate isomerase at 1.9 Å resolution. *Biochemistry,* **29**, 6609-6618.
Loria, J. P., Rance, M. & Palmer, A. G. (1999). A TROSY CPMG sequence for characterizing chemical exchange in large proteins. *J. Biomol. NMR,* **15**, 151-155.
Merritt, E. A. & Bacon, D. J. (1997). Raster3D: Photorealistic molecular graphics. *Methods Enzymol.* **277**, 505-524.
Minks, C., Huber, R., Moroder, L. & Budisa, N. (1999). Atomic mutations at the single tryptophan residue of human recombinant annexin V: effects on structure, stability, and activity. *Biochemistry,* **38**, 10649-10659.
Nickbarg, E. B. & Knowles, J. R. (1988). Triosephosphate isomerase: energetics of the reaction catalyzed by the yeast enzyme expressed in *Escherichia coli*. *Biochemistry,* **27**, 5939-5947.
Otwinowski, Z. & Minor, W. (1997). Processing of X-ray diffraction data collected in oscillation mode. *Methods Enzymol.* **276**, 307-326.
Parsons, J. F., Xiao, G. Y., Gilliland, G. L. & Armstrong, R. N. (1998). Enzymes harboring unnatural amino acids: mechanistic and structural analysis of the enhanced catalytic activity of a glutathione transferase containing 5-fluorotryptophan. *Biochemistry,* **37**, 6286-6294.
Plaut, B. & Knowles, J. R. (1972). pH-dependence of the triose phosphate isomerase reaction. *Biochem. J.* **129**, 311-320.
Pompliano, D. L., Peyman, A. & Knowles, J. R. (1990). Stabilization of a reaction intermediate as a catalytic device: definition of the functional role of the flexible loop in triosephosphate isomerase. *Biochemistry,* **29**, 3186-3194.
Putman, S. J., Coulson, A. F., Farley, I. R., Riddleston, B. & Knowles, J. R. (1972). Specificity and kinetics of triose phosphate isomerase from chicken muscle. *Biochem. J.* **129**, 301-310.
Richard, J. P. (1991). Kinetic parameters for the elimination reaction catalyzed by triosephosphate isomerase and an estimation of the reaction's physiological significance. *Biochemistry,* **30**, 4581-4585.
Rose, I. A., Fung, W. J. & Warms, J. V. (1990). Proton diffusion in the active-site of triosephosphate isomerase. *Biochemistry,* **29**, 4312-4317.
Rozovsky, S (2000). Triosephosphate isomerase: timescales of catalytic loop motion in relation to the rate limiting step. PhD thesis Columbia University, New York.
Rozovsky, S. & McDermott, A. E. (2001). The timescale of the catalytic loop motion in triosephosphate isomerase. *J. Mol. Biol.* **309**, 827-838.
Sampson, N. S. & Knowles, J. R. (1992a). Segmental motion in catalysis: investigation of a hydrogen bond critical for loop closure in the reaction of triosephosphate isomerase. *Biochemistry,* **31**, 8488-8494.
Sampson, N. S. & Knowles, J. R. (1992b). Segmental movement: definition of the structural requirements for loop closure in catalysis by triosephosphate isomerase. *Biochemistry,* **31**, 8482-8487.
Schneider, A. S. (2000). Triosephosphate isomerase deficiency: historical perspectives and molecular aspects. *Best Pract. Res. Clin. Haematol.* **13**, 119-140.
Taylor, H. C., Richardson, D. C., Richardson, J. S., Wlodawer, A., Komoriya, A. & Chaiken, I. M. (1981). Active conformation of an inactive semisynthetic ribonuclease-s. *J. Mol. Biol.* **149**, 313-317.
Webb, M. R., Standring, D. N. & Knowles, J. R. (1977). Phosphorus-31 nuclear magnetic resonance of dihydroxyacetone phosphate in the presence of triosephosphate isomerase. The question of nonproductive binding of the substrate hydrate. *Biochemistry,* **16**, 2738-2741.
Williams, J. C. & McDermott, A. E. (1995). Dynamics of the flexible loop of triosephosphate isomerase: the loop motion is not ligand gated. *Biochemistry,* **34**, 8309-8319.
Yuksel, K. U., Sun, A. Q., Gracy, R. W. & Schnackerz, K. D. (1994). The hinged lid of yeast triose-phosphate isomerase. Determination of the energy barrier between the two conformations. *J. Biol. Chem.* **269**, 5005-5008.

Edited by P. E. Wright

(Received 27 October 2000; received in revised form 28 March 2001; accepted 2 April 2001)